Structural Changes of *pharaonis* Phoborhodopsin upon Photoisomerization of the Retinal Chromophore: Infrared Spectral Comparison with Bacteriorhodopsin†

Hideki Kandori,*,‡ Kazumi Shimono,§ Yuki Sudo,§ Masayuki Iwamoto,§ Yoshinori Shichida,‡ and Naoki Kamo§

Department of Biophysics, Graduate School of Science, Kyoto University, Sakyo-ku, Kyoto 606-8502, Japan, and Laboratory of Biophysical Chemistry, Graduate School of Pharmaceutical Sciences, Hokkaido University, Sapporo 060, Japan

Received February 23, 2001; Revised Manuscript Received May 4, 2001

ABSTRACT: Archaeal rhodopsins possess a retinal molecule as their chromophores, and their light energy and light signal conversions are triggered by all-trans to 13-cis isomerization of the retinal chromophore. Relaxation through structural changes of the protein then leads to functional processes, proton pump in bacteriorhodopsin and transducer activation in sensory rhodopsins. In the present paper, low-temperature Fourier transform infrared spectroscopy is applied to phoborhodopsin from *Natronobacterium pharaonis* (*p*pR), a photoreceptor for the negative phototaxis of the bacteria, and infrared spectral changes before and after photoisomerization are compared with those of bacteriorhodopsin (BR) at 77 K. Spectral comparison of the C−C stretching vibrations of the retinal chromophore shows that chromophore conformation of the polyene chain is similar between *p*pR and BR. This fact implies that the unique chromophore−protein interaction in *p*pR, such as the blue-shifted absorption spectrum with vibrational fine structure, originates from both ends, the β-ionone ring and the Schiff base regions. In fact, less planer ring structure and stronger hydrogen bond of the Schiff base were suggested for *p*pR. Similar frequency changes upon photoisomerization are observed for the C=N stretch of the retinal Schiff base and the stretch of the neighboring threonine side chain (Thr79 in *p*pR and Thr89 in BR), suggesting that photoisomerization in *p*pR is driven by the motion of the Schiff base like BR. Nevertheless, the structure of the K state after photoisomerization is different between *p*pR and BR. In BR, chromophore distortion is localized in the Schiff base region, as shown in its hydrogen out-of-plane vibrations. In contrast, more extended structural changes take place in *p*pR in view of chromophore distortion and protein structural changes. Such structure of the K intermediate of *p*pR is probably correlated with its high thermal stability. In fact, almost identical infrared spectra are obtained between 77 and 170 K in *p*pR. Unique chromophore−protein interaction and photoisomerization processes in *p*pR are discussed on the basis of the present infrared spectral comparison with BR.

Halobacteria contain four retinal proteins (archaeal rhodopsins): bacteriorhodopsin (bR)[1] (*1*, *2*), halorhodopsin (hR) (*3*, *4*), sensory rhodopsin (sR) (*5*−*7*), and phoborhodopsin (pR)[2] (*8*, *9*). bR and hR are light-driven ion pumps, which act as an outward proton pump and an inward Cl^- pump, respectively (*1*, *2*, *4*). sR and pR are photoreceptors of this bacterium, which act for attractant and repellent responses in phototaxis, respectively (*7*, *10*). These four retinal proteins have similar structures; seven helices constitute the transmembrane portion of protein, and a retinal chromophore is bound to a lysine residue of the seventh helix via a protonated Schiff base linkage. Thus, functional differences presumably originate from the refined structural modification among them.

The level of understanding of the molecular mechanism in the four archaeal rhodopsins is highly different and roughly proportional to the amounts of these proteins in the cell membrane of *Halobacterium salinarum* (bR:hR:sR:pR = 1000:100:10:1). bR is one of the best understood membrane proteins. The tertiary structure of BR (light-adapted state having proton pump activity) and proton pathways in its pumping have been established, and detailed structural changes during the proton pump processes are investigated by various techniques (*1*, *2*, *11*−*14*). Structures of photointermediate states are also reported for BR_K (*15*), BR_L (*16*), and BR_M (*17*−*19*). In contrast, understanding of sensory rhodopsins such as sR and pR has been far behind.

pR has unique characteristics among the four archaeal rhodopsins. The absorption wavelength is 70−90 nm blue

† This work was supported in part by grants from the Japanese Ministry of Education, Culture, Sports, Science, and Technology, and by the Human Frontier Science Program.

* To whom correspondence should be addressed. Phone: 81-75-753-4211. Fax: 81-75-753-4210. E-mail: kandori@photo2.biophys.kyoto-u.ac.jp.

‡ Kyoto University.

§ Hokkaido University.

[1] Abbreviations: bR, bacteriorhodopsin; hR, halorhodopsin; sR, sensory rhodopsin; pR, phoborhodopsin; *p*pR, *pharaonis* phoborhodopsin; BR, light-adapted bacteriorhodopsin that has *all-trans*-retinal as its chromophore; BR_K, K intermediate of BR; BR_L, L intermediate of BR; BR_M, M intermediate of BR; pR_K, K intermediate of *pharaonis* phoborhodopsin; pR_L, L intermediate of *pharaonis* phoborhodopsin; pR_M, M intermediate of *pharaonis* phoborhodopsin; pR_O, O intermediate of *pharaonis* phoborhodopsin; FTIR, Fourier transform infrared; DM, *n*-dodecyl β-D-maltoside; PC, L-α-phosphatidylcholine; OG, octyl glucoside; HOOP, hydrogen out of plane.

[2] sR and pR are also called sensory rhodopsin-I (sR-I) and sensory rhodopsin-II (sR-II), respectively.

10.1021/bi0103819 CCC: $20.00
Published on Web 07/13/2001

shifted from other archaeal rhodopsins, so that pR looks orange (*20*−*23*). The absorption spectrum has a characteristic vibrational feature (*22*), whose mechanism has not been well understood. Although studies on pR had been difficult, successful purification of a pR-like protein from *Natronobacterium pharaonis*, a halophilic alkaliphilic bacterium, opened a new stage of investigation (*24*, *25*). Like pR, *pharaonis* phoborhodopsin (*p*pR) has an absorption maximum at about 500 nm with a characteristic spectral shoulder (*24*). The chromophore configuration is only all-trans in the dark state of *p*pR (*26*) as well as pR (*22*) and sR (*27*), whereas bR and hR have both all-trans and 13-cis forms. The photocycle intermediates are similar to those of BR, forming ppR$_K$, ppR$_L$, ppR$_M$, and ppR$_O$, whereas the photocycling rate of *p*pR is about 2 orders of magnitude longer than that of BR (*28*, *29*). It is known that ppR$_L$ is not trapped at low temperature and ppR$_K$ is highly stable (*24*, *30*).

Fourier transform infrared (FTIR) spectroscopy is a powerful tool in studying molecular structure and structural changes of retinal proteins, which has been proven for the study of BR (*12*, *13*, *31*−*33*). On the other hand, application of FTIR spectroscopy to pR and *p*pR has been much less reported so far. Engelhard et al. first reported the spectra of K-like and M-like species in *p*pR and observed protonation of a carboxylate upon M formation (*30*). On the other hand, Bergo et al. reported the spectra of O-like species in pR and revealed that Asp73 in pR (Asp85 in bR and Asp75 in *p*pR) is the proton acceptor of the retinal Schiff base (*34*). Despite such efforts, understanding of the molecular mechanism in *p*pR is still behind that of bR. In this paper, we applied low-temperature FTIR spectroscopy to *p*pR in the temperature range of 77−170 K, and the obtained spectra were compared with those of BR. On the basis of common and different spectral features, structure and structural changes upon photoisomerization of the retinal chromophore are compared between *p*pR and BR.

MATERIALS AND METHODS

Preparation of the ppR Sample. The plasmid including a full-length *psopII* with a fusing histidine tag was prepared by PCR. PCR was carried out using an oligonucleotide introducing a 3′-*Ava*I restriction site. The stop codon was deleted during amplification. The PCR product was ligated into pGEM-T easy. To construct the expression plasmid, pET/*p*pR His, the *Ava*I fragment from this plasmid was ligated to *Ava*I sites of pFE/ppR. This cloning strategy results in the following N- and C-terminal peptide sequence: ^{1}MVGL...AVAD^{240}**LEHHHHHH**.

DNA sequencing was carried out using a DNA sequencing kit (Applied Biosystems). All constructed plasmids were analyzed using an automated sequencer (377 DNA sequencer, Applied Biosystems).

The *p*pR protein was expressed in *Escherichia coli* BL21-(DE3) by induction by addition of 1 mM IPTG and 10 μM all-trans retinal. Preparation of crude membranes was described previously (*35*). The purification of *p*pR is essentially the same as that described in Hohenfeld et al. (*36*). Crude membranes were resuspended in buffer S (300 mM NaCl, 50 mM MES, 5 mM imidazole, pH 6.5) containing 1.5% *n*-dodecyl β-D-maltoside (DM) for 12 h at 4 °C. After centrifugation of the solubilized membranes (100000*g*) for 1.5 h at 4 °C, the supernatant was incubated with Ni−NTA agarose (Qiagen) for 1 h at room temperature with gentle stirring. The Ni−NTA resin was filled into a chromatography column and washed extensively with buffer W (0.1% DM, 300 mM NaCl, 50 mM MES, 50 mM imidazole, pH 6.5) to remove unspecifically bound proteins. The histidine-tagged proteins were eluted with buffer E (0.1% DM, 300 mM NaCl, 50 mM Tris-HCl, 150 mM imidazole, pH 7.0).

The purified *p*pR sample was then reconstituted into PC liposome. For reconstitution of L-α-phosphatidylcholine (egg, Avanti) lipids, 16 mg of PC lipids was dissolved in 800 μL of chloroform, and a thin lipid film on the wall of a 50 mL flask was prepared by careful evaporation of the solvent. Five milligrams of *p*pR in 8.5 mL of buffer E was added, and the suspension was gently stirred for 30 min at room temperature. The DM was removed by dialysis against 10 mM phosphate buffer (pH 7) containing 200 mM NaCl. The reconstitution protein was pelleted by ultracentrifugation at 300000*g*, 1 h, 4 °C.

FTIR Spectroscopy. FTIR spectroscopy was applied as described previously (*37*). Eighty microliters of the *p*pR sample in 2 mM phosphate buffer (pH 7.0) was dried on a BaF_2 window with a diameter of 18 mm. After hydration by either H_2O or D_2O, the sample was placed in a cell, mounted in an Oxford DN-1704 cryostat, and cooled to 77 K.

Illumination with 450 nm light at 77 K for 2 min converted *p*pR to ppR$_K$. Since the ppR$_K$ completely reverted to *p*pR upon illumination with >560 nm light for 1 min, as evidenced by the same but inverted spectral shape, the cycles of alternative illuminations with 450 nm light and >560 nm light were repeated a number of times. Other illumination conditions tested are with 420 nm light for conversion of *p*pR to ppR$_K$ and with >520 and >600 nm light for conversion of ppR$_K$ to *p*pR. The difference spectrum was calculated from the spectra constructed with 128 interferograms before and after the illumination. Twenty-four spectra obtained in this way were averaged for the ppR$_K$ minus *p*pR spectrum. The identical measurement was also conducted at 170 K. Linear dichroism experiments revealed a random orientation of the *p*pR molecules in the film. Therefore, an IR polarizer was not used in the measurements for *p*pR.

The BR$_K$ minus BR spectra were taken from Kandori et al. (*38*). The same sample (2 mM phosphate buffer, pH 7.0) was used for the measurements of the BR$_L$ minus BR spectra. The hydrated bR film was illuminated with >500 nm light for 1 min at 273 K to obtain the light-adapted state of bacteriorhodopsin (BR). The BR$_L$ minus BR spectra were obtained by illumination with >600 nm light for 2 min at 170 K (*39*, *40*). Five spectra constructed with 128 interferograms before and after the illumination were averaged for the BR$_L$ minus BR spectra. Since the bR molecules are highly oriented in the film, unlike *p*pR, the data with a window tilting angle of 53.5° in polarized FTIR spectroscopy were used for comparison.

RESULTS

Infrared Spectral Changes of ppR and BR at Low Temperature. In the present study, the *p*pR sample was

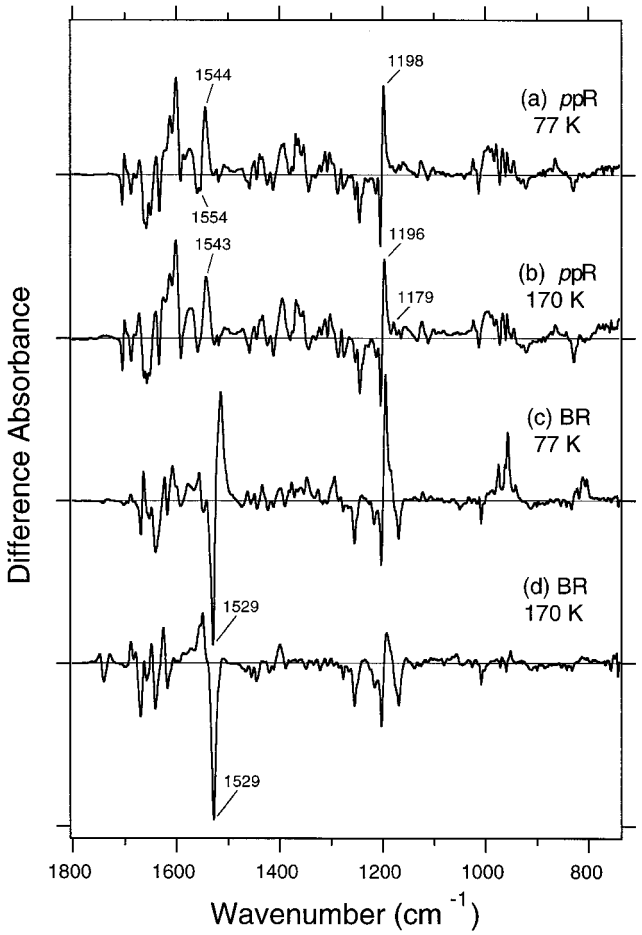

FIGURE 1: Difference infrared spectra of *p*pR at 77 K (a), *p*pR at 170 K (b), BR at 77 K (c), and BR at 170 K (d) in the 1800−740 cm^{-1} region. The spectra correspond to ppR_K minus *p*pR (a, b), BR_K minus BR (c), and BR_L minus BR (d). One division of the *y*-axis corresponds to 0.008 absorbance unit.

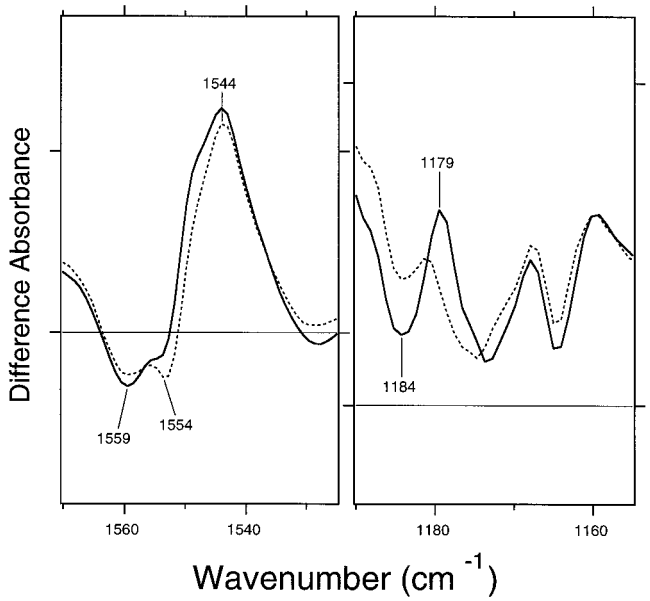

FIGURE 2: ppR_K minus *p*pR spectra under two different illumination conditions. After conversion of *p*pR to ppR_K with 450 nm light, *p*pR is reverted by illumination at >520 nm (solid line) and >600 nm (dotted line). The left panel corresponds to the frequency region of the C═C stretching vibration of the retinal chromophore. The right panel represents the frequency region of the only other difference between the two spectra. One division of the *y*-axis corresponds to 0.003 (left) and 0.001 (right) absorbance unit.

expressed in *E. coli*, solubilized by DM, purified by His tag, and reconstituted into PC liposome. Dry films were made from the PC liposome suspension and used for low-temperature FTIR spectroscopy after hydration. Visible absorption maxima of *p*pR in DM solution and in hydrated film were at 499 and at 497 nm, respectively, being similar to that of the native *p*pR in OG solution (498 nm) (*24*).

Figure 1 shows difference infrared spectra of *p*pR (a, b) and BR (c, d) measured at 77 and 170 K. BR_K and BR_L can be stabilized at 77 and 170 K, and spectra c and d in Figure 1 exhibit the typical BR_K minus BR and BR_L minus BR spectra, respectively (*12*). The most intense band is a negative band at 1529 cm^{-1}, which corresponds to ethylenic C═C stretching vibration of the retinal chromophore in BR. Lower and higher frequency shifts of this band in BR_K (c) and BR_L (d) indicate spectral red and blue shifts in visible absorption, respectively. Intense positive peaks in the 1000−900 cm^{-1} of BR_K (c) originate from hydrogen out-of-plane (HOOP) vibrations of the retinal chromophore, which significantly reduced in BR_L (d). This observation is interpreted in terms of the chromophore distortion in BR_K upon photoisomerization and its relaxation in BR_L. Clear spectral changes of BR_L, but not in BR_K, in the 1800−1700 cm^{-1} region show the structural changes of Asp96 and Asp115 (*12*). Thus, structural changes are localized around the retinal chromophore in BR_K, while the structural changes are extended into a wider region of the protein part in BR_L. Such observations were also confirmed by low-temperature X-ray crystallography of BR_K (*15*) and BR_L (*16*).

Unlike BR, infrared difference spectra of *p*pR are similar between 77 and 170 K (Figure 1a,b). Hirayama et al. reported that ppR_K is stable between 77 and 170 K by means of low-temperature visible absorption spectroscopy (*24*). Therefore, the present infrared spectra reproduced the previous observation for the native *p*pR dissolved in OG solution (*24*) and showed in addition that there are little changes in protein structures between 77 and 170 K.

Hirayama et al. also showed that ppR_K is composed of two species, whose difference absorption spectra with *p*pR have maxima at 525 and 535 nm (*24*). To examine the possibility of multiple K states, different illumination conditions are tested at 77 K. In Figure 2, *p*pR was first converted to ppR_K by illumination at 450 nm. Illumination at 420 nm displayed the identical infrared spectra (not shown), implying that *p*pR is composed of a single species in the original state. Then, ppR_K is reverted to the original *p*pR by illumination at >520 nm (solid line) or >600 nm (dotted line), the latter of which converts less 525 nm species to *p*pR. Figure 2 (left) shows the frequency region of the ethylenic C═C stretching vibration of the retinal chromophore, where the solid line has a reduced negative band at 1554 cm^{-1} and a positive band at 1544 cm^{-1} is considerably shifted to the higher frequency region. This fact indicates that ppR_K responding at >520 nm is blue shifted from ppR_K responding at >600 nm, being in agreement with the previous visible absorption (*24*).

Then we searched for differences in the infrared spectra between the two photoconversions, because infrared spectra are highly sensitive to molecular environment. Nevertheless, the two spectra were almost identical, indicating that two

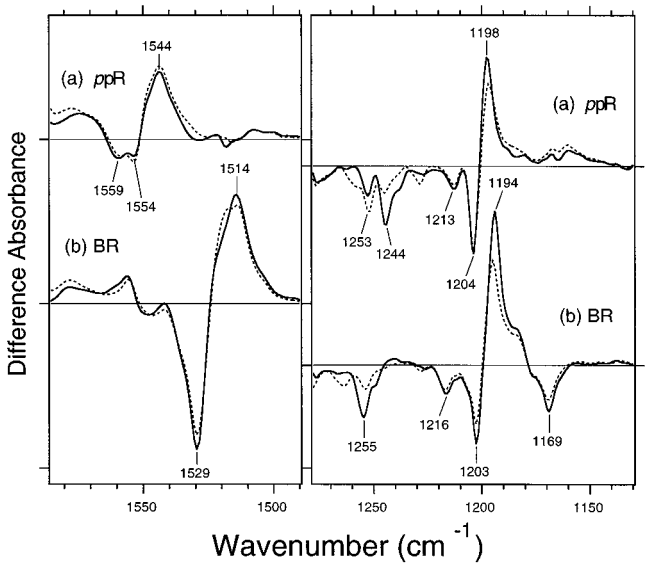

FIGURE 3: *p*pR$_K$ minus *p*pR (a) and BR$_K$ minus BR (b) spectra measured in the 1585−1490 (left) and 1280−1130 (right) cm^{-1} region at 77 K, which correspond to C═C and C−C stretching vibrations of the retinal chromophore, respectively. The sample was hydrated with either H_2O (solid lines) or D_2O (dotted lines). One division of the *y*-axis corresponds to 0.008 absorbance unit.

*p*pR$_K$ have nearly identical structures of the chromophore and its surrounding protein moiety. The only difference observed was the appearance of the 1184(−)/1179(+) cm^{-1} band in the photoconversion of 450 and >520 nm. This result suggests that the blue-shifted *p*pR$_K$ has a peak at 1179 cm^{-1}, while the red-shifted *p*pR$_K$ has the same peak as *p*pR at 1184 cm^{-1}. The band may originate from the C−C stretching vibration of the retinal chromophore.

The 1184(−)/1179(+) cm^{-1} band is also observed in the *p*pR$_K$ minus *p*pR spectrum at 170 K, as well as the lack of the negative 1554 cm^{-1} band (Figure 1b). This may also correspond to the two species of *p*pR$_K$, because Hirayama et al. showed the red-shifted *p*pR$_K$ decays at lower temperature than the blue-shifted *p*pR$_K$ (*24*). It is however noted that the spectral difference between 77 and 170 K (Figure 1a,b) is larger than that between the blue-shifted and red-shifted *p*pR$_K$ at 77 K. Thus, difference between spectra a and b in Figure 1 possibly originates from temperature effect due to local relaxation processes. In this paper, we compare the difference spectra at 77 K between *p*pR and BR, where the *p*pR$_K$ minus *p*pR spectra were obtained by photoconversion of 450 and >560 nm.

Comparison of the Vibrational Bands of the Retinal Chromophore between ppR and BR. Figure 3 shows the *p*pR$_K$ minus *p*pR (a) and BR$_K$ minus BR (b) spectra in the 1585−1490 (left) and 1280−1130 (right) cm^{-1} region. These frequency regions correspond to the C═C and C−C stretching vibrations of the retinal chromophore, respectively. In the former frequency region, there are two negative peaks at 1559 and 1554 cm^{-1} and a positive peak at 1544 cm^{-1} in *p*pR. The negative 1554 cm^{-1} band disappears at 170 K, whereas the other bands remained at 1558 cm^{-1} (−) and 1543 cm^{-1} (+) (Figure 1b). Such spectral feature is similar to the previous report for *p*pR in the native membrane at 170 K (*30*). These D_2O-insensitive bands presumably originate from the C═C stretching vibrations of the retinal chromophore. Previous resonance Raman spectroscopy of the native *p*pR in DM solution observed the C═C stretch at 1548 cm^{-1} (*41*).

Relatively small peaks of ethylenic C═C stretching vibrations are characteristic of *p*pR, which is in clear contrast to the results of BR (Figures 1 and 3). In BR, a strong peak pair is observed at 1529(−) and 1514(+) cm^{-1}. The results of BR have been interpreted in terms of a well-coupled symmetric C═C stretching mode in the planer chromophore structure. The planer chromophore structure is supported by the recent X-ray crystallography of BR (*42*, *43*). In this context, the smaller signal in *p*pR may originate from the lower coupling of the C═C stretching mode, possibly because of perturbation by the surrounding protein environment.

Negative bands in BR at 1255, 1216, 1203, and 1169 cm^{-1} are attributable for the C−C stretching vibrations of the retinal chromophore at positions C12−C13, C8−C9, C14−C15, and C10−C11, respectively (Figure 3b) (*12*, *44*). The negative 1255 cm^{-1} band is composed of a mixture of D_2O-insensitive C12−C13 stretching and D_2O-sensitive N−H in-plane bending vibrations (*45*). A positive 1194 cm^{-1} band of BR originates from C14−C15 and C10−C11 stretches (*46*). A similar spectral feature in *p*pR (Figure 3) suggests the similar chromophore conformations before and after photoisomerization. We tentatively assigned the bands at 1253(−), 1244(−), 1213(−), and 1204(−) cm^{-1} as the C12−C13 stretch, N−H bend, and C8−C9 and C14−C15 stretches in *p*pR. The remarkable difference in *p*pR is the lack of the negative band of BR at 1169 cm^{-1}. Since there is a peak around this frequency in the resonance Raman spectrum of *p*pR (*41*), it is likely to be no change for the C10−C11 frequency in *p*pR. In other words, the chromophore conformation is similar between *p*pR and BR, while its structural change upon photoisomerization is different at position C10−C11.

Figure 4 compares the spectra in the 1035−900 cm^{-1} region. It is well-known that hydrogen out-of-plane (HOOP) vibrations of the retinal chromophore appear in this region, and HOOP modes provide information of the chromophore distortion (*11*, *12*, *31*−*33*). The appearance of a sharp peak at 957 cm^{-1} is characteristic in the BR$_K$ minus BR spectrum, and bands at 974 and 957 cm^{-1} are sensitive to D_2O. They were assigned as HOOP vibrations of C15−H and N−H (*45*). This result indicates that the retinal distortion upon BR$_K$ formation is localized in the Schiff base region. In contrast, a more complex spectral feature was observed in *p*pR. Such spectral feature in the HOOP region did not depend on the illumination wavelengths. Namely, identical spectra were obtained by illumination at 420 nm instead of 450 nm for the *p*pR to *p*pR$_K$ conversion and by illuminations at >520 and >600 nm instead of >560 nm for the *p*pR$_K$ to *p*pR reversion (data not shown). Therefore, two *p*pR$_K$ species display identical HOOP bands. Identical frequencies were observed in the HOOP region at 170 K, though the amplitude of each band was somewhat different from 77 K (Figure 1).

Positive bands of *p*pR$_K$ at 966 and 958 cm^{-1} are insensitive to D_2O substitution. The half-amplitude of broad positive bands at 1001, 994, and 987 cm^{-1} remained in D_2O, suggesting that they are insensitive to D_2O and that the broad D_2O-sensitive band is also present in this region. A D_2O-sensitive 979 cm^{-1} band may originate from the C15− or N−HOOP mode. While the assignment of these HOOP

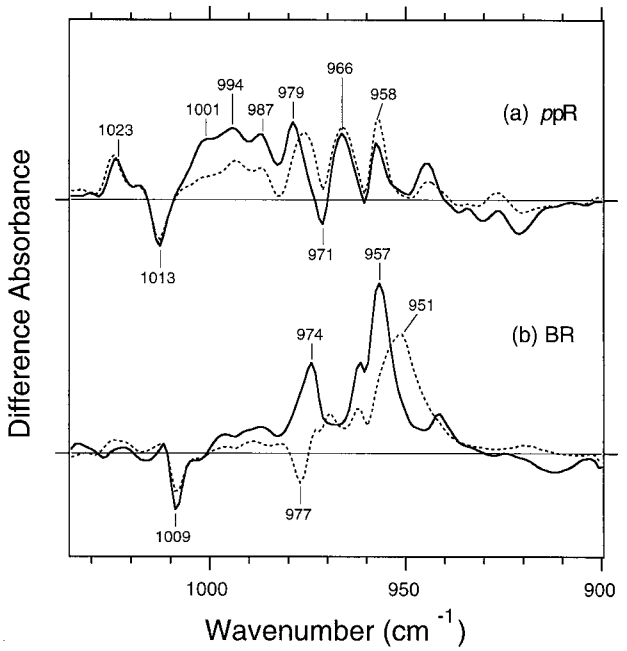

FIGURE 4: ppR_K minus *pp*R (a) and BR_K minus BR (b) spectra measured in the 1035−900 cm^{-1} region at 77 K, which correspond to hydrogen out-of-plane vibrations of the retinal chromophore. The sample was hydrated with either H_2O (solid lines) or D_2O (dotted lines). One division of the *y*-axis corresponds to 0.005 absorbance unit.

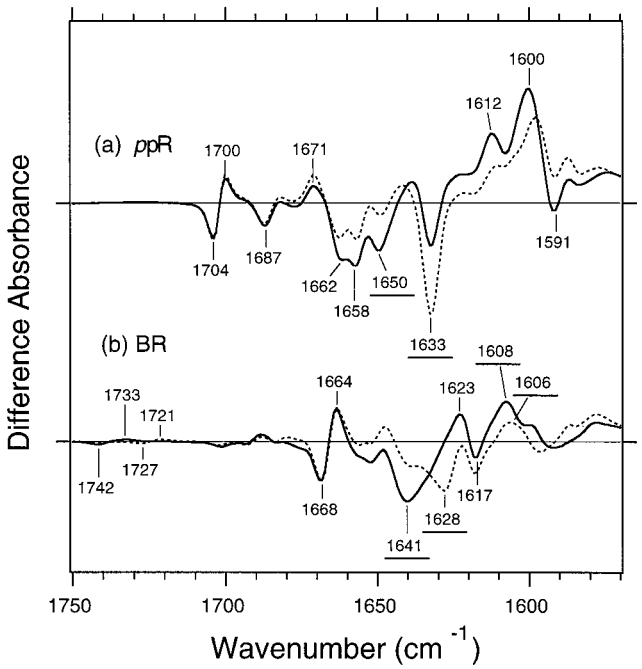

FIGURE 5: ppR_K minus *pp*R (a) and BR_K minus BR (b) spectra measured in the 1750−1570 cm^{-1} region at 77 K, most of which are ascribable for vibrations of protein. Underlined peaks are C═N stretching vibrations of the chromophore. The sample was hydrated with either H_2O (solid lines) or D_2O (dotted lines). One division of *y*-axis corresponds to 0.01 absorbance unit.

bands has to be done in the future, the clear appearance of the D_2O-insensitive HOOP modes in ppR_K implicates the specific chromophore distortion upon photoisomerization of *pp*R. Namely, chromophore distortion is localized at the Schiff base region in BR_K, while it is more extended into the other region in ppR_K.

Figure 5 shows the spectral changes in the 1750−1570 cm^{-1} region, where most signals originate from vibrations of protein. One exception is the C═N stretching vibration of the retinal Schiff base that appears in the 1650−1600 cm^{-1} region. In BR, the C═N stretch has been assigned at 1641 cm^{-1} in H_2O and at 1628 cm^{-1} in D_2O (Figure 5b) (*47*). The spectral upshift in H_2O is caused by the coupling of the N−H bending vibration of the Schiff base, and the difference in frequency between H_2O and D_2O has been regarded as the marker of hydrogen-bonding strength of the Schiff base (*48*−*50*). The small difference in BR_K (1608 cm^{-1} in H_2O and 1606 cm^{-1} in D_2O) has been interpreted in terms of the lack of a hydrogen bond in the Schiff base nitrogen after photoisomerization (*44*, *51*). Among various D_2O-sensitive bands of *pp*R (Figure 5a), negative bands at 1650 and 1633 cm^{-1} are likely to originate from the C═N stretches in H_2O and D_2O, respectively, because previous resonance Raman spectroscopy of the native *pp*R assigned at 1650 and 1627 cm^{-1}, respectively (*41*). Greater frequency difference in *pp*R than in BR [17 vs 13 cm^{-1} in the present FTIR spectroscopy and 23 (*41*) vs 17 cm^{-1} (*52*) from the previous resonance Raman spectroscopy] suggests a stronger hydrogen bond of the Schiff base in *pp*R. Regarding the C═N stretching mode of ppR_K, the positive 1612 cm^{-1} band is a candidate, which reduces the intensity in D_2O. If the small band at around this frequency in D_2O is the C═N stretch of ppR_K, lack of the hydrogen bond upon photoisomerization is identical to the case in BR.

The present spectral comparison of the chromophore vibrations provided various aspects between *pp*R and BR. As shown in the C−C stretches of the original state (Figure 3), chromophore conformation is similar in the polyene chain, suggesting that *pp*R possesses planer polyene structure like BR. Nevertheless, mode coupling in the C═C stretch is less in *pp*R (Figure 3). In BR, the C5═C6 bond is also involved in the same plane of the other double bonds (*42*, *43*). Thus, less mode coupling in *pp*R may be caused by the structural difference at the β-ionone ring moiety from BR. In the original state, the hydrogen bond of the Schiff base is stronger in *pp*R than in BR. In the K state after photoisomerization, lack of the hydrogen bond of the Schiff base seems to be common between *pp*R and BR (Figure 5). Nevertheless, appearance of the HOOP modes was highly different between them (Figure 4), implying different chromophore distortion in the K state. In BR_K, chromophore distortion is localized at the Schiff base region, as shown in D_2O-sensitive HOOP modes. A more complex feature involving D_2O-insensitive bands implies that the chromophore distortion is extended into the other part in ppR_K (Figure 4). The structural difference observed for the C10−C11 stretch (Figure 3) may be related to the HOOP results.

Comparison of the Vibrational Bands of the Protein Moiety between ppR and BR. The other bands than the C═N stretch of the Schiff base are from protein in Figure 5. In BR, the 1742(−)/1733(+) cm^{-1} bands in H_2O are shifted to 1727(−)/1721(+) cm^{-1} in D_2O, which was previously assigned as the C═O stretch of Asp115 (*53*). The corresponding amino acid is Asn105 in *pp*R, so that no spectral changes are observed in the 1750−1710 cm^{-1} region of *pp*R (Figure 5a). The 1623(+)/1617(−) cm^{-1} bands of BR were previously assigned as the C═O stretch of the peptide carbonyl (amide I vibration) of Val49 (*54*), which is located

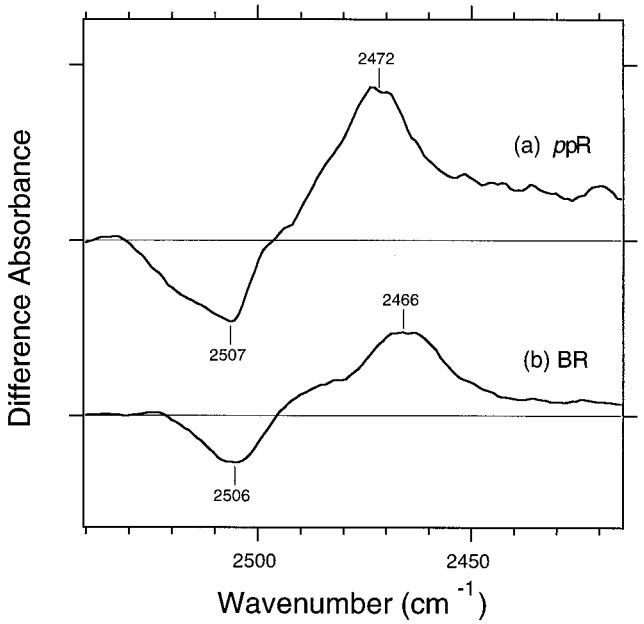

FIGURE 6: ppR_K minus *p*pR (a) and BR_K minus BR (b) spectra measured in the 2540−2415 cm^{-1} region at 77 K. The sample was hydrated with D_2O, and the 2506(−)/2466(+) bands of BR (b) were previously assigned to the O−D stretching vibration of threonine at position 89 (*56*). One division of the *y*-axis corresponds to 0.0008 absorbance unit.

close to the Schiff base. The 1668(−)/1664(+) cm^{-1} bands are highly dichroic (*38*) and appear in the typical frequency region of the amide I vibration of the αII helix (*55*), which is probably located in the transmembrane region.

In *p*pR, the following bands were observed in the 1750−1570 cm^{-1} region: 1704(−), 1700(+), 1687(−), 1671(+), 1662(−), 1658(−), 1650(−), 1633(−), 1612(+), 1600(+), and 1591(−) cm^{-1}. The 1671(+)/1662(−) cm^{-1} bands appeared in the typical frequency region of the amide I vibration of the αII helix. The 1658 cm^{-1} band appears in the amide I vibration of the α-helix (αI helix). The 1704(−)/1700(+) cm^{-1} bands are considerably higher than the amide I vibration, which may be ascribable for C═O stretching vibration of asparagine. In fact, the corresponding amino acid to Asp115 of BR (Figure 5b) is Asn105 in *p*pR. The positive band at 1600 cm^{-1} is the greatest peak in the ppR_K minus *p*pR spectrum (Figure 1), and the corresponding negative one is presumably at 1591 cm^{-1} (Figure 5). The half-amplitude of the peaks is lost in D_2O. The negative peak at 1633 cm^{-1} in H_2O and D_2O indicates that protein vibration is involved in this band in addition to the C═N stretch of the retinal chromophore. Thus, relatively many protein bands are observed for *p*pR in comparison with that of BR.

Figure 6 shows the spectral changes in the O−D stretching vibrational region. In BR, the 2506(−)/2466(+) cm^{-1} bands were assigned as the O−D stretching vibrations of Thr89 (Figure 6b) (*56*). The O−D stretching frequency of BR at 2506 cm^{-1} indicates a strong hydrogen bond of Thr89 with Asp85. The O−D stretch of BR_K at 2466 cm^{-1} is lower than that of the neat liquid alcohol (*56*), indicating a further strengthened hydrogen bond. We interpreted the change in hydrogen bond due to strong association between Thr89 and Asp85, which is caused by retinal isomerization. Similar spectral changes are observed at 2507(−)/2472(+) cm^{-1} in *p*pR, too (Figure 6a). Since *p*pR possesses the corresponding threonine and aspartate (Thr79 and Asp75), it is likely that the hydrogen-bonding conditions of Thr79 and Asp75 in *p*pR are similar to those in BR, and photoisomerization causes similar structural changes in the region.

DISCUSSION

Chromophore−Protein Interaction in ppR and BR. The spectral comparison of the C−C stretching vibrations of the retinal chromophore (Figure 3) revealed that the conformation of the polyene in *p*pR is similar to that in BR. Since BR has a planer polyene chain (*42*, *43*), it is likely that *p*pR also has a planer structure of the polyene chain. This fact implies that the central part of the chromophore does not contribute to the significant differences of *p*pR from BR in view of (i) vibrational fine structure, (ii) spectral blue shift, and (iii) isomer selectivity. In other words, the differences are likely to originate from both ends of the chromophore, namely, the β-ionone ring and/or the Schiff base regions.

In general, polyenes exhibit vibrational fine strutcure in their absorption spectra. Thus, lack of the fine structure in the absorption spectrum of BR has been extensively discussed (*11*, *57*), where inhomogeneous and/or homogeneous spectral broadening in the BR chromophore destroys the structure. Weakened interactions between the Schiff base proton and its counterion were proposed to destabilize the geometry in the Schiff base environmnet, which increases the fluctuations in the distance between the counterion and the proton (*22*, *58*). Alternatively, similar inhomogeneous broadening could occur at the other end of the β-ionone ring (*22*, *58*). The present results show that hydrogen bonding of the Schiff base is stronger in *p*pR than in BR (Figure 5), which support the origin from the Schiff base region.

As the origin of the vibrational fine structure unique for the absorption spectrum of *p*pR, the restricted retinal binding pocket involving the β-ionone ring has been proposed to lower the degree of freedom in the chromophore motion (*59*, *60*). The present results suggest that the restricted portion in *p*pR is not at the polyene chain. In BR, the C5═C6 bond of the β-ionone ring is involved in the same plane of the other double bonds, which forms a planer 6-s-trans conformation (*42*, *43*). Previous experiments using retinal analogues revealed that pR (*61*) possesses a 6-s-trans conformation like BR. Despite no report for *p*pR, a similar absorption property suggests that *p*pR has a 6-s-trans conformation, too. This fact may suggest that the structure around the β-ionone ring is similar between *p*pR and BR. It is however noted that mode coupling in the C═C stretch is less in *p*pR than in BR (Figure 3), suggesting that the 6-s-trans conformation is less planer in *p*pR.

Regarding the comparison between *p*pR and BR, the BR structure (*42*, *43*) provides useful information, because the recent projection structure showed that *p*pR has similar structure at 6.9 Å resolution as BR (*62*). Figure 7 shows 10 amino acids that are different between BR and *p*pR among 25 amino acid residues within 5 Å from the retinal chromophore in BR.[3] As is seen in Figure 7, the difference in amino acids is mainly localized around the β-ionone ring.

[3] The corresponding 25 amino acids of BR are as follows: Met20, Val49, Ala53, Tyr57, Tyr83, Asp85, Trp86, Thr89, Thr90, Leu93, Asp115, Met118, Ile119, Gly122, Trp138, Ser141, Thr142, Met145, Trp182, Tyr185, Pro186, Trp189, Asp212, Ala215, and Lys216.

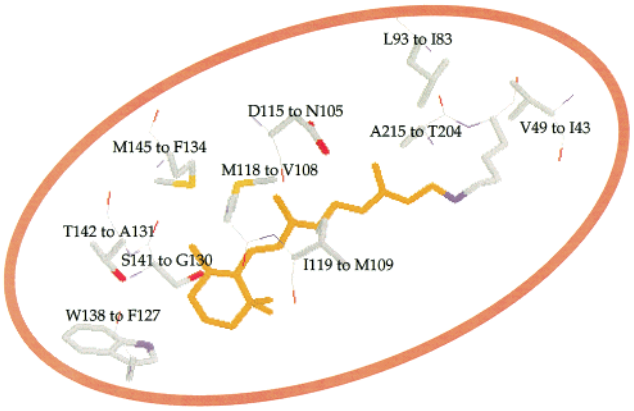

FIGURE 7: X-ray crystallographic structures of BR (*42*). Among 25 amino acid residues within 5 Å from the retinal chromophore, 10 amino acids are shown that are different between bR (written in the former) and *p*pR (written in the latter). The difference is more localized at the β-ionone ring portion.

In particular, amino acids in helices D (Asn105, Val108, and Met109 in *p*pR) and E (Phe127, Gly130, Ala131, and Phe134 in *p*pR) must be closely related to the specific structure around the β-ionone ring in *p*pR. Shimono et al. replaced two amino acids of *p*pR (Val108 and Gly130) around the β-ionone ring to those of bR (Met, and Ser, respectively), which exhibits reduced vibrational fine structure, accompanying spectral red shift by 10 nm (*63*). Thus, it is likely that both the β-ionone ring and Schiff base regions contribute the vibrational fine structure in the absorption spectrum of *p*pR.

Both ends of the retinal chromophore also appear to contribute an absorption maximum in the 480−500 nm region, which is characteristic of *p*pR and pR. Less mode coupling in the C=C stretch in *p*pR than in BR (Figure 3), presumably because of less planer 6-s-trans conformation, can explain such spectral blue shift of *p*pR from other archaeal rhodopsins. In addition, stronger hydrogen bonding of the Schiff base in *p*pR than in BR is consistent with the spectral blue shift in *p*pR, where the stronger interaction between the retinyl cation and the counterion leads to charge localization in the Schiff base region. The present study revealed that the spectral shift of *p*pR$_K$ by 10 nm (525 and 535 nm species) can be achieved under very limited structural alteration (Figure 2). This fact implies highly sensitive feature of electronic absorption of the retinal chromophore.

Unlike the β-ionone ring moiety, the Schiff base side is considerably conserved between *p*pR and bR (Figure 7). In addition, the present FTIR study suggested that the hydrogen-bonding interaction between Thr89 and Asp85 in BR (*56*) is also preserved for Thr79 and Asp75 in *p*pR (Figure 6). These facts suggest that the structure of the Schiff base region is essentially similar between *p*pR and BR. Therefore, stronger hydrogen bonding of the Schiff base in *p*pR than in BR may originate from small changes in hydrogen-bonding networks involving water molecules. In this regard, it is of interest to study the water structure in the Schiff base region, which is our next focus.

Photoisomerization Mechanism and Property of the K Intermediates in ppR and BR. In the K state after photoisomerization, lack of a hydrogen bond of the Schiff base seems to be common between *p*pR and BR (Figure 5). In addition, a strengthened hydrogen bond of the threonine side

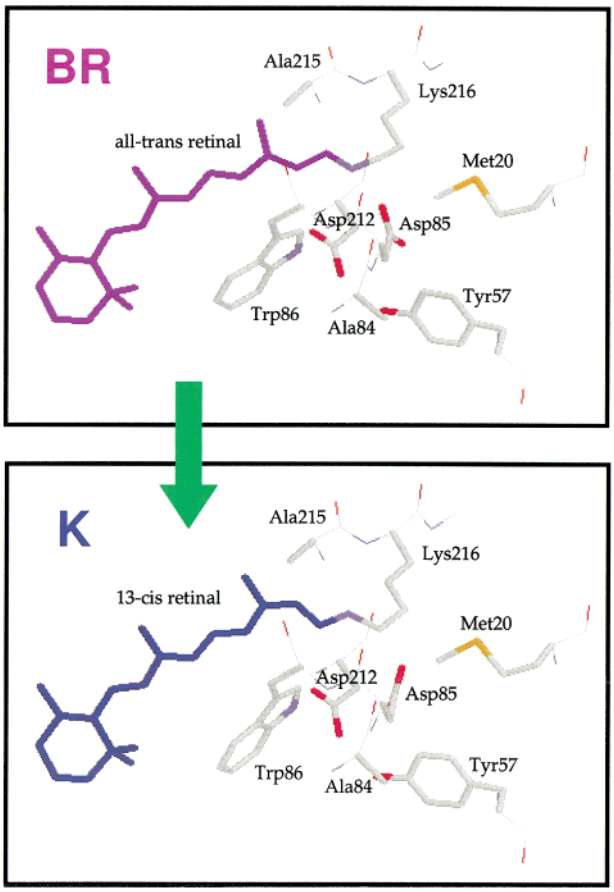

FIGURE 8: X-ray crystallographic structures of BR (upper) and BR$_K$ (lower) measured at 110 K (*15*). Shown are amino acids whose structures are changed between them. It is noted that the structural changes are localized at the Schiff base region, and the amino acid residues except for Ala215 are conserved in *p*pR (Figure 7).

chain at positions 89 in BR and 79 in *p*pR is likely to be common between them. Thus, structural changes of the Schiff base region accompanying retinal photoisomerization are suggested to be the same between BR and *p*pR. Nevertheless, the appearance of the HOOP modes was highly different between them (Figure 4), which implies different chromophore distortion in the K state. Chromophore distortion is localized at the Schiff base region in BR$_K$, while it is extended into the other part in *p*pR$_K$. In addition, more protein bands are observed in *p*pR than in BR (Figure 5). These facts suggest that structural changes upon formation of the K state are globally extended in *p*pR than in BR.

In the case of BR, the X-ray crystallographic structure was already reported for BR$_K$ (*15*). Figure 8 shows the amino acids whose structures are changed between BR and BR$_K$. It is noted that the amino acid residues shown are not all ones to change structures, because our FTIR study observed changes in hydrogen bonds of the side chains of three

[4] In addition, the structural model of BR$_K$ (*15*) contradicts with our FTIR results (*56*) in view of the hydrogen-bonding alteration of Thr89. The X-ray crystallographic structure of BR$_K$ suggests no motion of Thr89 and rotation of the side chain of Asp85, resulting in cleavage of the hydrogen bond between the side chains of Thr89 and Asp85 upon photoisomerization (*15*). In contrast, the FTIR study assigned the O−D stretch of Thr89 in D_2O, and interpreted stronger association between the side chains of Thr89 and Asp85 upon photoisomerization (*56*). Therefore, the BR$_K$ structure may be questioned in view of local interaction.

threonines; Thr17, Thr89, and Thr121 (or Thr90) (*56*, *64*).[4] This fact can be interpreted by the difference in resolution; namely, vibrational bands are more sensitive to structural changes, and the amino acids shown in Figure 8 are likely to exhibit greater structural rearrangement in BR_K. As is seen, the changed amino acids are localized into one side of the C13═C14 double bond. The structure suggests that the other side (β-ionone ring and polyene chain) has greater mass so that it is difficult to move. Therefore, the Schiff base side actually rotates, which accompanies rearrangement of the hydrogen- bonding network. Localized structural changes of the Schiff base region in BR, as shown in the HOOP bands (Figure 4), must be the result of such change.

Figure 8 shows that the changed amino acid residues are conserved in *p*pR except for Ala215 (Figure 7). This fact and similar spectral changes of the Schiff base and Thr79 in *p*pR (Figures 5 and 6) suggest rotation of the Schiff base region in *p*pR, too. However, the HOOP bands are extended into the other region than the Schiff base in *p*pR (Figure 4). Different chromophore−protein interaction at the β-ionone ring and the Schiff base region could yield different chromophore distortion after photoisomerization. The quantum yield of photoisomerization in *p*pR has been reported to be 0.5 (*65*), while that of BR is known to be 0.6−0.65 (*66*, *67*). An essentially similar quantum yield of *p*pR suggests similar photoisomerization processes to those of BR. On the other hand, the slightly lower value may be related to the extended structural changes of the retinal chromophore, because smaller motion through the excited state appears to result in greater product formation.

The extended protein structural changes in *p*pR are probably correlated with the thermal stability of ppR_K and lack of ppR_L at low temperature. It is known that ppR_K is stable and ppR_L is not trapped at low temperature (*24*), though ppR_L is formed at room temperature (*29*). In BR, light energy is locally converted into the structural constraint at the Schiff base region. Increase in temperature accompanies extended protein structure by relaxing the constraint, in the BR_K to BR_L transition (Figure 1c,d). In contrast, structural constraint is already relaxed in ppR_K, which accompanies extended protein structural changes.

ACKNOWLEDGMENT

We thank Dr. M. Sumi for various discussions.

REFERENCES

1. Lanyi, J. K. (1997) *J. Biol. Chem. 272*, 31209−31212.
2. Haupts, U., Tittor, J., and Oesterhelt, D. (1999) *Annu. Rev. Biophys. Biomol. Struct. 28*, 367−399.
3. Matsuno-Yagi, A., and Mukohata, Y. (1977) *Biochem. Biophys. Res. Commun. 78*, 237−243.
4. Lanyi, J. K. (1990) *Physiol. Rev. 70*, 319−330.
5. Bogomolni, R. A., and Spudich, J. L. (1982) *Proc. Natl. Acad. Sci. U.S.A. 79*, 6250−6254.
6. Tsuda, M., Hazemoto, N., Kondo, M., Kamo, N., Kobatake, Y., and Terayama, Y. (1982) *Biochem. Biophys. Res. Commun. 108*, 970−976.
7. Hoff, W. D., Jung, K. H., and Spudich, J. L. (1997) *Annu. Rev. Biophys. Biomol. Struct. 26*, 223−258.
8. Takahashi, T., Tomioka, H., Kamo, N., and Kobatake, Y. (1985) *FEMS Microbiol. Lett. 28*, 161−164.
9. Zhang, W., Brooun, A., Mueller, M. M., and Alam, M. (1996) *Proc. Natl. Acad. Sci. U.S.A. 93*, 8230−8235.
10. Sasaki, J., and Spudich, J. L. (2000) *Biochim. Biophys. Acta 1460*, 230−239.
11. Mathies, R. A., Lin, S. W., Ames, J. B., and Pollard, W. T. (1991) *Annu. Rev. Biophys. Biophys. Chem. 20*, 491−518.
12. Maeda, A. (1995) *Isr. J. Chem. 35*, 387−400.
13. Kandori, H. (2000) *Biochim. Biophys. Acta 1460*, 177−191.
14. Subramaniam, S., and Henderson, R. (2000) *Biochim. Biophys. Acta 1460*, 157−165.
15. Edman, K., Nollert, P., Royant, A., Belrhali, H., Pebay-Peyroula, E., Hajdu, J., Neutze, R., and Landau, E. M. (1999) *Nature 401*, 822−826.
16. Royant, A., Edman, K., Ursby, T., Pebay-Peyroula, E., Landau, E. M., and Neutze, R. (2000) *Nature 406*, 645−648.
17. Luecke, H., Schobert, B., Richter, H.-T., Cartailler, J.-P., and Lanyi, J. K. (1999) *Science 286*, 255−260.
18. Luecke, H., Schobert, B., Cartailler, J.-P., Richter, H.-T., Rosengarth, A., Needleman, R., and Lanyi, J. K. (2000) *J. Mol. Biol. 300*, 1237−1255.
19. Sass, H. J., Büldt, G., Gessenich, R., Hehn, D., Neff, D., Schlesinger, R., Berendzen, J., and Ormos, P. (2000) *Nature 406*, 649−653.
20. Tomioka, H., Takahashi, T., Kamo, N., and Kobatake, Y. (1986) *Biochem. Biophys. Res. Commun. 139*, 389−395.
21. Shichida, Y., Imamoto, Y., Yoshizawa, T., Takahashi, T., Tomioka, H., Kamo, N., and Kobatake, Y. (1988) *FEBS Lett. 236*, 333−336.
22. Takahashi, T., Yan, B., Mazur, P., Derguini, F., Nakanishi, K., and Spudich, J. L. (1990) *Biochemistry 29*, 8467−8474.
23. Imamoto, Y., Shichida, Y., Yoshizawa, T., Tomioka, H., Takahashi, T., Fujikawa, K., Kamo, N., and Kobatake, Y. (1991) *Biochemistry 30*, 7416−7424.
24. Hirayama, J., Imamoto, Y., Shichida, Y., Kamo, N., Tomioka, H., and Yoshizawa, T. (1992) *Biochemistry 31*, 2093−2098.
25. Scharf, B., Pevec, B., Hess, B., and Engelhard, M. (1992) *Eur. J. Biochem. 206*, 359−366.
26. Imamoto, Y., Shichida, Y., Hirayama, J., Tomioka, H., Kamo, N., and Yoshizawa, T. (1992) *Biochemistry 31*, 2523−2528.
27. Yan, B., Nakanishi, K., and Spudich, J. L. (1991) *Proc. Natl. Acad. Sci. U.S.A. 88*, 9412−9416.
28. Miyazaki, M., Hirayama, J., Hayakawa, M., and Kamo, N. (1992) *Biochim. Biophys. Acta 1140*, 22−29.
29. Imamoto, Y., Shichida, Y., Hirayama, J., Tomioka, H., Kamo, N., and Yoshizawa, T. (1992) *Photochem. Photobiol. 56*, 1129−1134.
30. Engelhard, M., Scharf, B., and Siebert, F. (1996) *FEBS Lett. 395*, 195−198.
31. Rothschild, K. J. (1992) *J. Bioenerg. Biomembr. 24*, 147−167.
32. Siebert, F. (1995) *Methods Enzymol. 246*, 501−526.
33. Gerwert, K. (1999) *Biol. Chem. 380*, 931−935.
34. Bergo, V., Spudich, E. N., Scott, K. L., Spudich, J. L., and Rothschild, K. J. (2000) *Biochemistry 39*, 2823−2830.
35. Shimono, K., Iwamoto, M., Sumi, M., and Kamo, N. (1997) *FEBS Lett. 420*, 54−56.
36. Hohenfeld, I. P., Wegener, A. A., and Engelhard, M. (1999) *FEBS Lett. 442*, 198−202.
37. Kandori, H., and Maeda, A. (1995) *Biochemistry 34*, 14220−14229.
38. Kandori, H., Kinoshita, N., Shichida, Y., and Maeda, A. (1998) *J. Phys. Chem. B 102*, 7899−7905.
39. Yamazaki, Y., Sasaki, J., Hatanaka, M., Kandori, H., Maeda, A., Needleman, R., Shinada, T., Yoshihara, K., Brown, L. S., and Lanyi, J. K. (1995) *Biochemistry 34*, 577−582.
40. Kandori, H., Yamazaki, Y., Sasaki, J., Needleman, R., Lanyi, J. K., and Maeda, A. (1995) *J. Am. Chem. Soc. 117*, 2118−2119.
41. Gellini, C., Luttenberg, B., Sydor, J., Engelhard, M., and Hildebrandt, P. (2000) *FEBS Lett. 472*, 263−266.

42. Luecke, H., Schobert, B., Richter, H.-T., Cartailler, J. P., and Lanyi, J. K. (1999) *J. Mol. Biol. 291*, 899−911.
43. Belrhali, H., Nollert, P., Royant, A., Menzel, C., Rosenbusch, J. P., Landau, E. M., and Pebay-Peyroula, E. (1999) *Structure 7*, 909−917.
44. Smith, S. O., Lugtenburg, J., and Mathies, R. A. (1985) *J. Membr. Biol. 85*, 95−109.
45. Maeda, A., Sasaki, J., Pfefferlé, J.-M., Shichida, Y., and Yoshizawa, T. (1991) *Photochem. Photobiol. 54*, 911−921.
46. Gerwert, K., and Siebert, F. (1986) *EMBO J. 5*, 805−811.
47. Siebert, F., and Mäntele, W. (1983) *Eur. J. Biochem. 130*, 565−573.
48. Aton, B., Doukas, A. G., Callender, R. H., Dinur, U., and Honig, B. (1980) *Biophys. J. 29*, 79−94.
49. Rodman-Gilson, H. S., Honig, B., Croteau, A., Zarrilli, G., and Nakanishi, K. (1988) *Biophys. J. 53*, 261−269.
50. Baasov, T., Friedman, N., and Sheves, M. (1987) *Biochemistry 26*, 3210−3217.
51. Rothschild, K. J., Roepe, P., Lugtenburg, J., and Pardoen, J. A. (1984) *Biochemistry 23*, 6103−6109.
52. Diller, R., Stockburger, M., Oesterhelt, D., and Tittor, J. (1987) *FEBS Lett. 217*, 297−304.
53. Braiman, M. S., Mogi, T., Marti, T., Stern, L. J., Engel, F., Khorana, H. G., and Rothschild, K. J. (1988) *Biochemistry 27*, 8516−8520.
54. Yamazaki, Y., Tuzi, S., Saitô, H., Kandori, H., Needleman, R., Lanyi, J. K., and Maeda, A. (1996) *Biochemistry 35*, 4063−4068.
55. Krimm, S., and Dwivedi, A. M. (1982) *Science 216*, 407−409.
56. Kandori, H., Kinoshita, N., Yamazaki, Y., Maeda, A., Shichida, Y., Needleman, R., Lanyi, J. K., Bizounok, M., Herzfeld, J., Raap, J., and Lugtenburg, J. (1999) *Biochemistry 38*, 9676−9683.
57. Birge, R. R. (1990) *Biochim. Biophys. Acta 1016*, 293−327.
58. El-Sayed, M. A., Karvaly, B., and Fukumoto, J. M. (1981) *Proc. Natl. Acad. Sci. U.S.A. 78*, 7512−7516.
59. Hirayama, J., Imamoto, Y., Shichida, Y., Yoshizawa, T., Asato, A. E., Liu, R. S., and Kamo, N. (1994) *Photochem. Photobiol. 60*, 388−393.
60. Hirayama, J., Kamo, N., Imamoto, Y., Shichida, Y., and Yoshizawa, T. (1995) *FEBS Lett. 364*, 168−170.
61. Wada, A., Akai, A., Goshima, T., Takahashi, T., and Ito, M. (1998) *Bioorg. Med. Chem. Lett. 8*, 1365−1368.
62. Kunji, E. R. S., Spudich, E. N., Grisshammer, R., Henderson, R., and Spudich, J. L. (2001) *J. Mol. Biol. 308*, 279−293.
63. Shimono, K., Iwamoto, M., Sumi, M., and Kamo, N. (2000) *Photochem. Photobiol. 72*, 141−145.
64. Kandori, H., Kinoshita, N., Yamazaki, Y., Maeda, A., Shichida, Y., Needleman, R., Lanyi, J. K., Bizounok, M., Herzfeld, J., Raap, J., and Lugtenburg, J. (2000) *Proc. Natl. Acad. Sci. U.S.A. 97*, 4643−4648.
65. Losi, A., Wegener, A. A., Engelhard, M., Gartner, W., and Braslavsky, S. E. (1999) *Biophys. J. 77*, 3277−3286.
66. Tittor, J., and Oesterhelt, D. (1990) *FEBS Lett. 263*, 269−273.
67. Zhang, H., and Mauzerall, D. (1996) *Biophys. J. 71*, 381−388.

BI0103819